Toxicology Reports 1 (2014) 188–199

Contents lists available at ScienceDirect

Toxicology Reports

journal homepage: www.elsevier.com/locate/toxrep

In vitro anticancer drug test: A new method emerges from the model of glioma stem cells

Gabriele Riva [a], Simona Baronchelli [a,b], Laura Paoletta [a], Valentina Butta [a], Ida Biunno [b,c], Marialuisa Lavitrano [a], Leda Dalprà [a,d], Angela Bentivegna [a,*]

[a] Department of Surgery and Translational Medicine, University of Milano-Bicocca, via Cadore 48, 20900 Monza, Italy
[b] Institute for Genetic and Biomedical Research - National Research Council (IRGB-CNR), via Fantoli 16/15, 20138 Milan, Italy
[c] IRCCS MultiMedica, Science and Technology Pole, via Fantoli 16/15, 20138 Milan, Italy
[d] Medical Genetics Laboratory, S. Gerardo Hospital, via Pergolesi 33, 20900 Monza, Italy

ARTICLE INFO

Article history:
Received 19 February 2014
Received in revised form 8 May 2014
Accepted 12 May 2014
Available online 22 May 2014

Keywords:
Glioma stem cells (GSCs)
In vitro drug sensitivity test
Paclitaxel
Valproic acid
Differentiation therapy

ABSTRACT

Glioblastoma multiforme (GBM) is a grade IV astrocytoma and the most common malignant brain tumor. Current therapies provide a median survival of 12–15 months after diagnosis, due to the high recurrence rate. The failure of current therapies may be due to the presence, within the tumor, of cells characterized by enhanced self-renewal capacity, multilineage differentiation potential and elevated invasive behavior, called glioma stem cells (GSCs). To evaluate the pharmacological efficacy of selected drugs on six GSC lines, we set up a multiple drug responsivity assay based on the combined evaluation of cytomorphological and functional parameters, including the analysis of polymorphic nuclei, mitotic index and cell viability. In order to understand the real pharmacological efficacy of the tested drugs, we assigned a specific drug responsivity score to each GSC line, integrating the data produced by multiple assays. In this work we explored the antineoplastic effects of paclitaxel (PTX), an inhibitor of microtubule depolymerization, utilized as standard treatment in several cancers, and of valproic acid (VPA), an inhibitor of histone deacetylases (HDACs) with multiple anticancer properties. We classified the six GSC lines as responsive or resistant to these drugs, on the basis of their responsivity scores. This method can also be useful to identify the best way to combine two or more drugs. In particular, we utilized the pro-differentiating effect of VPA to improve the PTX effectiveness and we observed a significant reduction of cell viability compared to single treatments.

1. Introduction

Glioblastoma multiforme (GBM) is the most frequent and aggressive primary tumor of the central nervous system, defined as grade IV astrocytoma (WHO classification) [40]. Despite aggressive multimodal therapies, such as surgical resection, chemo- and radiotherapy, the median survival of patients remains about 12 months, because of rapid tumor recurrence [62]. The differences in drug sensitivity, even in the same histological type of tumor, could be explained by the extremely heterogeneous landscape of genetic alterations and gene expression patterns of GBM [65,25,26]. On the other hand, an explanation for resistance both to radiation and chemotherapy and eventual tumor relapse was imputed to specific tumor cells endowed with stem-like properties, the glioma stem

* Corresponding author at: Department of Surgery and Translational Medicine, University of Milano-Bicocca, via Cadore 48, 20900 Monza, Italy. Tel.: +39 0264488133; fax: +39 0264488253.
E-mail address: angela.bentivegna@unimib.it (A. Bentivegna).

http://dx.doi.org/10.1016/j.toxrep.2014.05.005

cell (GSC) subpopulation [47,38,39]. Evidences prove that GSC lines represent a valuable biological *in vitro* model of GBM, as they are more representative of the respective primary tumor [35]. GSCs are characterized by an enhanced self-renewal capacity and a severe impairment of the differentiation potential, due to a permanent epigenetic block [2,58]. These findings suggest the crucial importance of the development of GSC-targeted therapy in order to specifically eradicate the stem cell compartment of the tumor. Overcoming the differentiation block could constitute an interesting therapeutic strategy [53].

Recently, the lack of consistency in cell viability data obtained in different laboratories on the same cell lines treated with the same compounds has underlined the importance of simultaneously evaluating multiple cell parameters to carefully determine the pharmacological effectiveness of the tested drugs [3,19,21,61].

Aim of this study was to develop a novel drug responsivity multiple assay based on the combined evaluation of cytomorphological and functional parameters to assess the pharmacological effectiveness of the tested drugs. In particular, we investigated both morphological and cytogenetic parameters, directly or indirectly involved in the cytotoxic action of the tested molecules, such as polymorphic nuclei and mitotic index, in addition to cell viability. The different biological nature of these data required the formulation of a method to evaluate them simultaneously in order to understand the real pharmacological efficacy of the tested compounds. In this work, we used, as example of antineoplastic drugs, paclitaxel (PTX), an antimitotic drug [13], and valproic acid (VPA), an anticonvulsant and mood-stabilizing drug [15], on six GSC lines. These compounds are both used in treatment and management of several cancers and are different in their molecular activities: VPA is a histone deacetylases (HDAC) inhibitor, while PTX is an inhibitor of microtubule depolimerization. Our multiple drug responsivity assay has proven itself useful in identifying how to best carry out a combined treatment of these two drugs. In fact we evaluated the therapeutic advantage of a sequential treatment with VPA followed by PTX in comparison with the treatment with a single drug. We advanced a therapeutic strategy based on the chemosensitization of GSCs, determined by the induction of cellular differentiation, and the consequent treatment with a standard antiproliferative drug.

2. Materials and methods

2.1. Cell lines and cell culture conditions

The six GSC lines used in this work (GBM2, GBM7, G144, G166, G179 and GliNS2) have been isolated from patients affected by GBM [20,45] and in 2013, our research group characterized their cytogenomic and epigenomic profiles [2]. The stemness properties of the GSC lines were periodically monitored, as already described [2]. Cells were cultured in adherent culture condition using 10 μg/ml laminin (Invitrogen) in a proliferation permissive medium composed by DMEM F-12 and Neurobasal 1:1 (Invitrogen), B-27 supplement without vitamin A (Invitrogen), 2 mM L-glutamine, 10 ng/ml recombinant human bFGF and 20 ng/ml recombinant human EGF (Miltenyi Biotec), 20UI/ml penicillin and 20 μg/ml streptomycin (Euroclone) (complete medium).

2.2. Drugs and treatments

Valproic acid (sodium salt, Sigma) was dissolved in sterile water to a stock concentration of 50 mg/ml and stored at −20 °C. Paclitaxel (Lc laboratories) was dissolved in absolute ethanol to 10 mM stock concentration and then diluted to the required concentrations, with complete cell culture medium. The final concentration of ethanol was no greater than 0.1%. This concentration of solvent had no effect on cell viability (measured by MTT assay). Dose–response studies were carried out in order to determine the suitable doses for further experiments. Cell culture treatments were assessed following two different schedules of administration: (i) single drug treatment was performed using 0.5–1–3–6–10–20 mM VPA or 0.01–0.1–1–10–20–50 μM PTX for 24, 48 and 72hs and (ii) dual drug treatment was performed treating cells with different concentrations of VPA for 24 h and then adding PTX at different concentrations for 48 h (Fig. S1).

Supplementary Fig. 1 can be found, in the online version, at doi:10.1016/j.toxrep.2014.05.005.

2.3. Cytomorphological analysis

Cells were seeded in T-25 cm^3 at a concentration of 0.4×10^6 cell/ml. When cells reached the 80% confluence, they were treated with 2 mM VPA or with 10 μM PTX for 24 and 48hs. Subsequently, chromosomal preparations were performed by means of standard procedures as previously described [2]. Briefly, chromosomes were QFQ-banded using quinacrine mustard and slides were mounted in McIlvaine buffer. Slides were analyzed using Nikon Eclipse 80i fluorescence microscope (Nikon) (60× magnification) equipped with a COHU High Performance CCD camera. Cytomorphological parameters were analyzed using preparations derived from the same cell passage. Mitotic index and polymorphic nuclei were evaluated counting the percentage of mitosis and aberrant nuclei, scoring at least 1000 nuclei. Data were obtained as mean values, derived from two independent experiments using cells at different passages.

For the cellular morphological study, cells were seeded in 6-well plates without laminin coating in proliferative permissive medium at 3×10^3–10^4 cells/ml, depending on the growth rate of each cell line, and after 24 h, cells were treated with VPA (0.5–1–6–10 mM) or PTX (0.1–1–10–20–50 μM) concentrations for different times of exposure (24, 48 and 72 h). The presence of morphological changes was estimated through the observation at phase contrast microscopy, comparing VPA or PTX-treated and untreated cells. Representative images were taken for each cell line and for each treatment.

2.4. Whole chromosome painting FISH

FISH was performed on interphasic nuclei using Whole Chromosome Painting (WCP) probes. Particularly, we

utilized the Octochrome Chromoprobe Multiprobe System (Cytocell, Cambridge, UK) and procedures were performed according to the manufacturer's protocol. A minimum of 100 nuclei was evaluated for each specific square.

2.5. Immunofluorescence

The immunofluorescence assays were performed on untreated and 2 mM VPA-treated cultures for 72 h. The experiments were performed on all GSC lines using rabbit anti-CD133 (Santa Cruz Biotechnology, Santa Cruz, CA, USA; 1:50), mouse anti-nestin (Millipore, Billerica, MA, USA; 1:50), rabbit anti-glial fibrillary acidic protein (GFAP, Dako, 1:200), rabbit anti-βIII tubulin (Covance, 1:100) and goat anti-Myelin basic protein (MBP, Santa Cruz Biotechnology, 1:50) as primary antibodies. Cells were placed onto slides by means of Cytospin, washed with Dulbecco's modified phosphate-buffered saline (PBS), fixed with 4% paraformaldehyde for 15 min and treated for 10 min with 0.1 M glycine (in PBS). Slides were incubated 30 min at room temperature (RT) in blocking solution (5% Bovine serum albumin, BSA, 0.6% Triton X-100 in PBS) and treated for 30 minutes with 70 U/mg RNAse (Sigma–Aldrich, Milan, Italy; 1:30) in blocking solution. Cells were incubated with the primary antibodies at 4 °C overnight. Then, slides were rinsed with washing buffer (0.3% Triton X-100 in PBS) and incubated with secondary fluorescent antibodies and 2.5 mg/ml propidium iodide (PI) for 1 h at RT. Alexa Fluor 488-conjugated goat anti-mouse or anti-rabbit and donkey anti-goat (Molecular Probes Eugene, OR, USA; 1:200) were used as secondary antibodies. Alexa Fluor 647-conjugated phalloidin (Molecular Probes, Eugene, OR, USA; 1:200) was used to visualize the actin filaments. Then, cells were washed with PBS and coverslips were mounted using Polyvinyl alcohol mounting medium (Fluka Analytical, Milan, Italy). Fluorescent cell preparations were examined using a Radiance 2100 confocal microscope (Bio-Rad, Hercules, CA, USA). Noise reduction was achieved by Kalman filtering during acquisition. In order to perform a semi-quantitative analysis, the number of immunoreactive cells was counted, evaluating at least 100 cells per sample over different areas of the slide. Staining intensity was classified in 5 categories: negative (−; 0–20% of immunoreactive cells); marginal (±; 21–40%); low (+; 41–60%); medium (++; 61–80%); and high (+++; 81–100%)[37]. Any statistical significant difference between treated and untreated cells was evaluated by Fishers exact test on raw data.

2.6. Cell viability

MTT assays were performed to evaluate the efficacy of antineoplastic drugs. Cells were seeded at a density of 2–4 × 10^4 cells/well in a 96-well-plate in 100 μL of culture medium and incubated at 37 °C. We treated cells at passages similar to the ones used for cytomorphological analysis. After 24 h, drugs were added to complete cell culture medium at various concentrations. After the drug incubation time (24, 48, 72 h), MTT solution (0.5 mg/ml, Sigma) was added to each well and incubated for 3 h at 37 °C. Therefore, formazan was solubilized in absolute ethanol. The absorbance of the dye was measured spectrophotometrically at a 595 nm wavelength using an automated microplate reader (Bio-Rad). The percentage of inhibition was determined by comparing the absorbance values of drug-treated cells with that of untreated controls: [(treated-cell absorbance/untreated cell absorbance) × 100]. The results reported are the mean values of two different experiments performed at least in triplicate.

2.7. Cooperative index

To evaluate the effects of combined VPA-PTX treatment, the Cooperative Index (CI) was calculated comparing the sum of cell death percentages obtained for each single agent to the percentage of cell death upon combined treatment (CI = VPA cell death% + PTX cell death%/Combined treament cell death%). CI values < 1 indicate a synergistic effect, CI values = 1 an additive effect, while CI values > 1 indicate an antagonistic effect [1].

2.8. Statistical analysis

Statistical analysis was performed using chi-square, Fisher's exact test or *t*-test on raw data, by means of Excel spreadsheet (Microsoft Office 2007, Microsoft Corporation) or OpenEpi software v2.3.1, available online at http://www.openepi.com/. The critical level of significance was set at $p < 0.05$.

3. Results

3.1. Cell viability after single treatments with VPA or PTX

The effect of VPA and PTX on the cell viability of the GSC lines was determined by MTT assay (Fig. S1A). The inhibitory effect on viability of both drugs was heterogeneous among the six cell lines. VPA treatment inhibited cell viability in a dose- and time-dependent manner in all the GSC lines. As shown in Fig. 1, GBM2 was the most sensitive cell line to VPA treatment, showing a decrease in cell viability at all doses after 48 h and 72 h treatments, while after 24 h cells were only sensitive at the highest doses of the drug. The other five GSC lines showed a consistent reduction in cell viability only at 72 h of 20 mM VPA treatment. PTX was less effective than VPA, in fact five out of six cell lines were relatively resistant to PTX treatment and a considerable inhibition of metabolic activity (GBM7 40%, G144 20%, G166 26%, G179 32% and GliNS2 30%) was observed only at the highest concentration (50 μM) and after the longest time of treatment (72 h). GBM2 cell line, instead, exhibited the greatest inhibitory effect on cell viability after PTX treatment, mainly at 48–72 h of exposure: for example, PTX 50 μM for 72 h induced a significant decrease in cell viability of approximately 70% (Fig. 1, Table S1).

Supplementary Table 1 can be found, in the online version, at doi:10.1016/j.toxrep.2014.05.005.

Since for therapeutic purposes it is important to use the lowest possible pharmacological concentration to minimize side effects, for all subsequent experiments we decided to use an intermediate VPA dose (2 mM). This

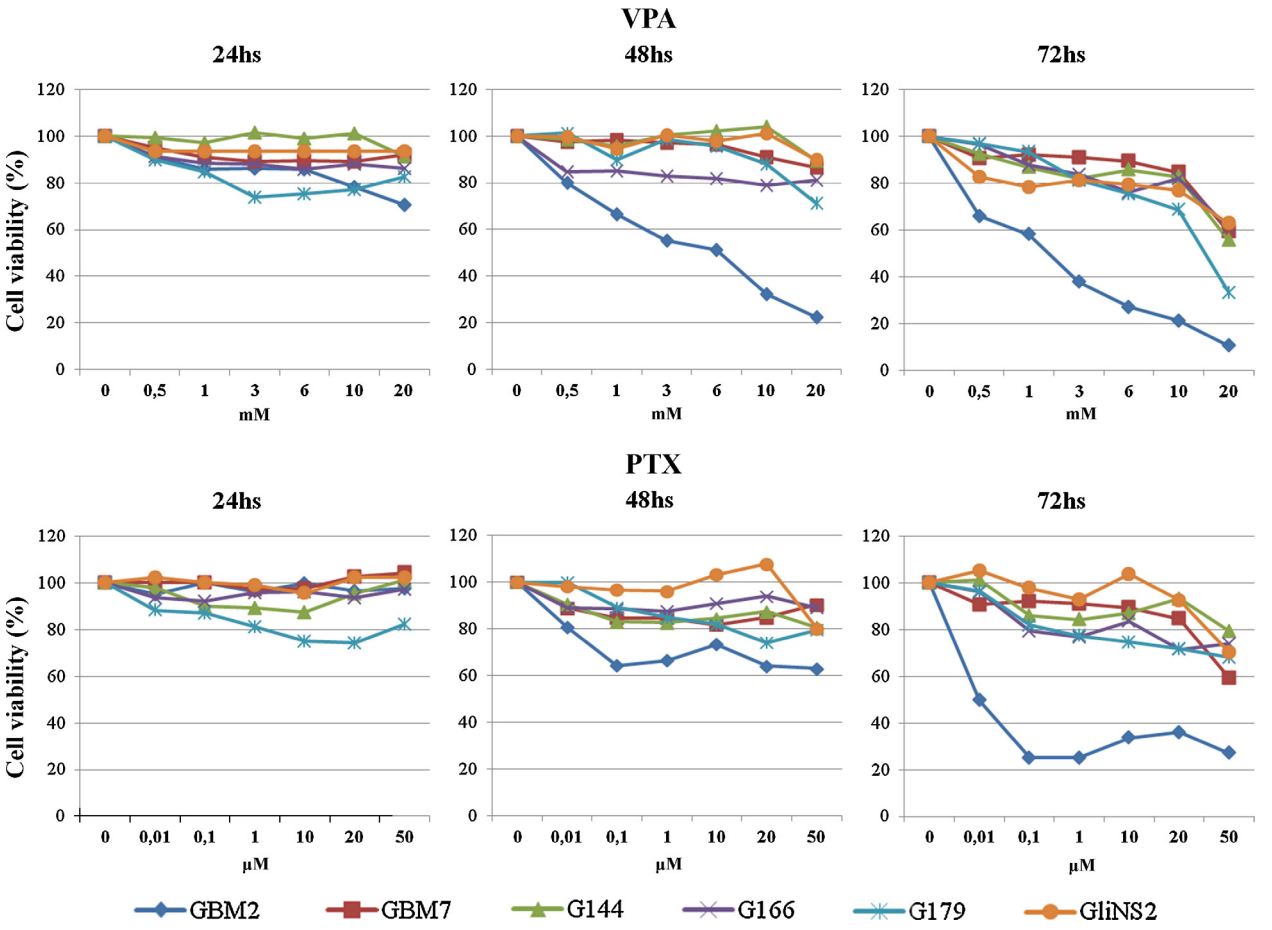

Fig. 1. Cell viability assays on GSC lines using VPA and PTX in single treatment. Cell viability was measured as percentage of cell survival in drug-treated cells relative to untreated cells. Results are reported as means from two different experiments performed at least in triplicate. Standard error of the mean (SEM) was constantly lower than 5% of each mean value.

concentration was set as a consequence of the observation, after 24 h treatment, of a shift in cell viability and a diversification of drug susceptibility among the cell lines raising the dose from 1 mM (no effect) to 3 mM (effect). Regarding to PTX concentration, we selected a 10 μM dose, because, after 24 h of treatment, it allowed the maximum reduction of viability in all the cell lines (Fig. 1).

3.2. Polymorphic nuclei

The presence of aberrant nuclei, which are a hallmark of cancer, was evidenced in all the GSC lines analyzed, either treated or untreated. The nuclear shapes were irregular, various and resembled the aberrant nuclear structures of GBM histological preparations (Fig. S2A), thus representing a typical cancer-related feature. We observed donut-shaped, ring-shaped, polylobate and fragmented nuclei, nuclei with multiple blebs and the remarkable presence of micronuclei (Fig. S2B).

Supplementary Fig. 2 can be found, in the online version, at doi:10.1016/j.toxrep.2014.05.005.

After PTX treatment, the presence of defective mitotic figures, such as uncondensed chromatin threads, chromosome fragmentation and de-condensed chromosomes, arranged in nuclei-like structures was noticed (Fig. S2C). Chi-square test was assessed to identify any statistically significant difference between treated and untreated cells (Table S2). The statistical analysis allowed us to categorize GSC lines in two main groups. The first group included GBM7, G144, G166 and G179 cell lines: they showed a very high percentage of polymorphic nuclei in untreated cells (80–90%) and, therefore, a shift in the percentage of aberrant nuclei after drug exposure could not be appreciated. The second group was represented by GBM2 and GliNS2 cell lines, which had a low percentage of polymorphic nuclei in untreated cells (approximately 15% and 10%, respectively). In this group, both VPA and PTX induced a significant increase in polymorphic nuclei at 24 (except for GliNS2 line treated with VPA) and 48 h of treatment, compared to the corresponding untreated cells (Fig. 2, Table S2). After PTX administration, the increment of polymorphic nuclei was time-dependent and higher than after VPA administration (Fig. 2, Table S2).

Supplementary Table 2 can be found, in the online version, at doi:10.1016/j.toxrep.2014.05.005.

To confirm that the figures observed referred to aberrant nuclei and were not the consequence of entosis-like mechanisms [31], we performed chromosome preparations

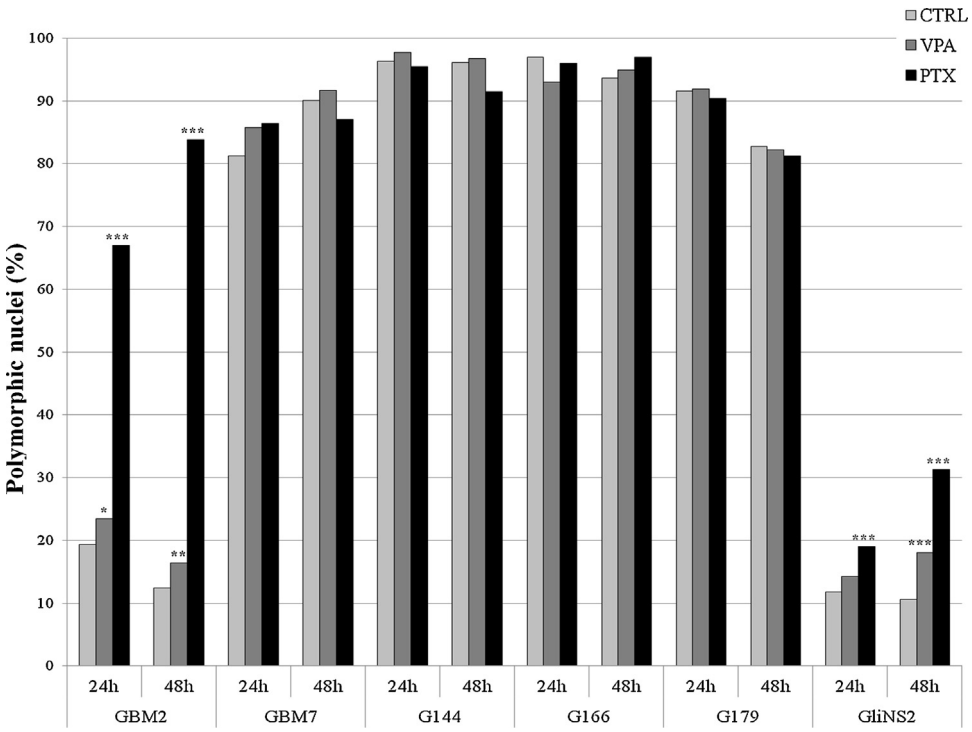

Fig. 2. Percentages of polymorphic nuclei in VPA or PTX treated and untreated cells. Chi-square test, treated *vs.* untreated cells: $^{*}p < 0.05$; $^{**}p < 0.001$; $^{***}p < 0.0001$.

without the use of hypotonic solution, in order to preserve the original nuclear architecture. We found that the nuclear aberrant shapes were almost maintained by the corresponding metaphases (Fig. S3 – top), demostrating that the several nuclear structures within a cell, including nuclear fragments and micronuclei, synchronically undergo mitosis, thus excluding the presence of entosis-like mechanisms.

Supplementary Fig. 3 can be found, in the online version, at doi:10.1016/j.toxrep.2014.05.005.

In order to rule out the possible preferential localization of each chromosome in micronuclei and/or nuclear fragments, FISH analysis was performed on interphasic nuclei of untreated cells using WCP probes. As shown in Fig. S3 – bottom, we observed a random chromosome localization within these aberrant structures, suggesting the lack of specific patterns.

3.3. Mitotic index

The mitotic activity is a crucial parameter to measure the aggressiveness of a tumor and it is therefore associated with important clinical implications. To study the effects of VPA and PTX exposure on cellular proliferation, we evaluated the mitotic index (MI) in chromosome preparations. VPA administration determined a decrease of MI in all the cell lines analyzed both at 24 and 48 h of treatment, while PTX determined a time-dependent decrease of MI only in GliNS2 and G179 cell lines (Fig. 3). PTX had no effect on G144 and GBM7 cell lines, while, in the G166 cell line, it significantly reduced the MI only after 48 h of exposure. GBM2 cell line showed a peculiar behavior: the 24 h administration induced a considerable accumulation of metaphases, but this trend reversed after 48 h, when MI resulted significantly decreased if compared to untreated cells.

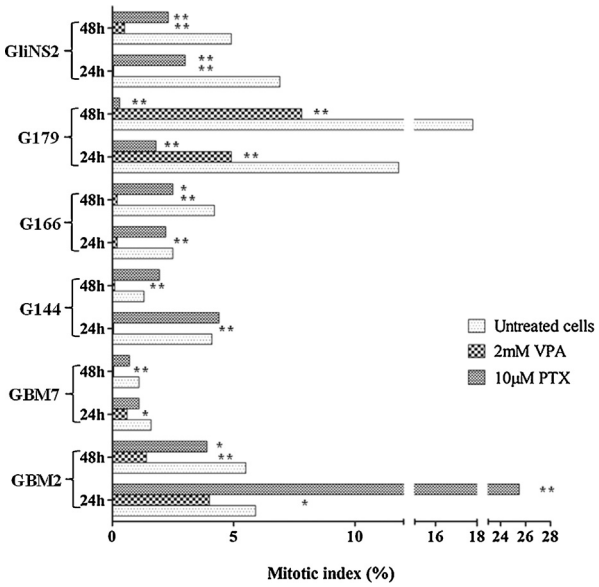

Fig. 3. VPA and PTX effects on mitotic index of GSC lines. Results are reported as percentages, resulting from means of two independent experiments. Chi-square test on raw data: $^{*}p < 0.05$; $^{**}p < 0.0001$.

Table 1
Drug responsivity index. In the table below, we reported the scores (from −3 to +3) assigned to *p*-values of all the experiments, evaluating also the therapeutic goodness of the specific data expressed by algebraic signs (+ or −), performed in order to obtain a final index of drug sensibility for each cell line.

Cell lines	Mitotic index				Polymorphic nuclei				MTT				Drug responsivity index	
	VPA		PTX		VPA		PTX		VPA[a]		PTX[b]		VPA 24/48 h	PTX 24/48 h
	24 h	48 h	24 h	48 h	24 h	48 h	24 h	48 h	24 h	48 h	24 h	48 h		
GBM2	+1	+3	−3	+1	−1	−2	−3	−3	+1	+3	0	+3	5	−5
GBM7	+1	+3	0	0	0	0	0	0	0	0	0	+1	4	1
G144	+3	+3	0	0	0	0	0	0	0	0	0	+1	6	1
G166	+3	+3	0	+1	0	0	0	0	+2	+1	0	0	9	1
G179	+3	+3	+3	+3	0	0	0	0	0	0	0	+1	6	7
GliNS2	+3	+3	+3	+3	0	−3	−3	−3	0	0	0	0	3	0

Legend: 1, −1: $p < 0.05$; 2, −2: $p < 0.001$; 3, −3: $p < 0.0001$; 0, not statistically significant; score ≥ 1, responsive; score ≤ 0, resistant.
[a] Vpa 3 mM.
[b] PTX 10 μM.

3.4. Multiple drug responsivity assay

In order to assess the pharmacological efficacy of the tested compounds, we developed a rapid, inexpensive and simple method that allowed us to combine the data obtained through the analysis of different parameters. We assigned a score (from 1 to 3) to each parameter, depending on *p*-values: specifically, we attributed the score of 1, 2 or 3 to *p*-value < 0.05, 0.001 or 0.0001, respectively. Moreover, in order to suggest an interpretation of the therapeutic goodness of the results we assigned a positive or negative sign to each score. In particular, a statistically significant reduction of cell viability, MI and polymorphic nuclei percentages were considered as good events for therapeutic purposes and we assigned them positive values of the score. Conversely, increases in these parameters were interpreted as unfavorable events for therapeutic purposes and their scores were negative. The scores obtained from the 24 and 48 h treatments were added together in order to indicate the cell line's general susceptibility to the drug and the algebraic sum of the scores obtained from the three parameters represents its drug responsivity index.

G144, G166 and G179 lines had the highest VPA responsivity indexes (6, 9 and 6, respectively) suggesting a significant sensitivity to this drug; the other lines displayed a more modest response to VPA.

With regard to PTX, G179 line reached a high score (7), demonstrating a strong susceptibility to the drug. GBM2 and GliNS2 lines showed scores which suggested their resistance to PTX (-5 and 0, respectively), while the others were weakly responsive (Table 1).

3.5. Cellular morphology

VPA and PTX effects on the six GSC lines were also evaluated at morphological level. GSCs were seeded as described in Section 2 and, after 24 h, they were treated with several concentrations of VPA or PTX. Matching untreated cells were used as control. Subsequently, both cultures were observed with a phase contrast microscope at different time points (24–48–72 h). GSCs of untreated controls grew in non-adherent growth pattern as neurosphere.

VPA treatment determined drastic morphological changes in all the GSC lines, compared to controls. Cells modified their morphology from round spheres to adherent cells. Most cells were star-shaped with cellular astrocytic-like processes indicating a pro-differentiating effect of VPA. In particular, GBM2, G179 and GliNS2 lines showed differentiated-like morphology changes after 24 h treatment with the lowest pharmacological concentration (0.5 mM). Regarding the G144 line, the first morphological variations were appreciable after 48 h of exposure to 1 mM VPA. Finally, GBM7 and G166 lines began to differentiate when exposed to 6 mM VPA. It should be noted that the highest concentrations of VPA (6 mM and 10 mM) caused, at the longest time of exposure, the appearance of dead cells and large quantities of cellular debris in GBM2 and G179 cell lines (Fig. S4).

Supplementary Fig. 4 can be found, in the online version, at doi:10.1016/j.toxrep.2014.05.005.

As expected, PTX-treated GSCs did not show any relevant morphological variations (data not shown).

3.6. Analysis of stemness and differentiation markers by immunofluorescence

The pro-differentiating ability of VPA was evaluated through the expression analysis of selected stemness (CD133 and Nestin) and differentiation markers (GFAP, β III tubulin and MBP), that have been previously used in literature [24,57,36,45], comparing untreated cells *versus* 2 mM-72 h VPA treated cells. The overview of data showed that GSCs expressed both stemness and differentiation markers at variable levels. Generally, Nestin was expressed at medium or high intensity in all untreated cell lines (range: 63.1–99.2%). CD133 immunoreactive cells were found as a large proportion of untreated GSCs in 5/6 cell lines (62.7–100%). Only G166 cell line showed almost a negative expression of this marker (only 7.3% of CD133+ cell). Untreated cells of all GSC lines were also variously positive for differentiation markers. Thus, an aberrant co-expression of differentiation markers with stem/progenitor markers was not rare: in fact, the tumor sphere population is heterogeneous and GSC cultures recapitulate *in vitro* the hierarchical organization of tumor itself, being composed by stem-like, transient amplifying progenitors and differentiated cancer cells [57]. VPA treatment caused a change in the percentage of cells positive

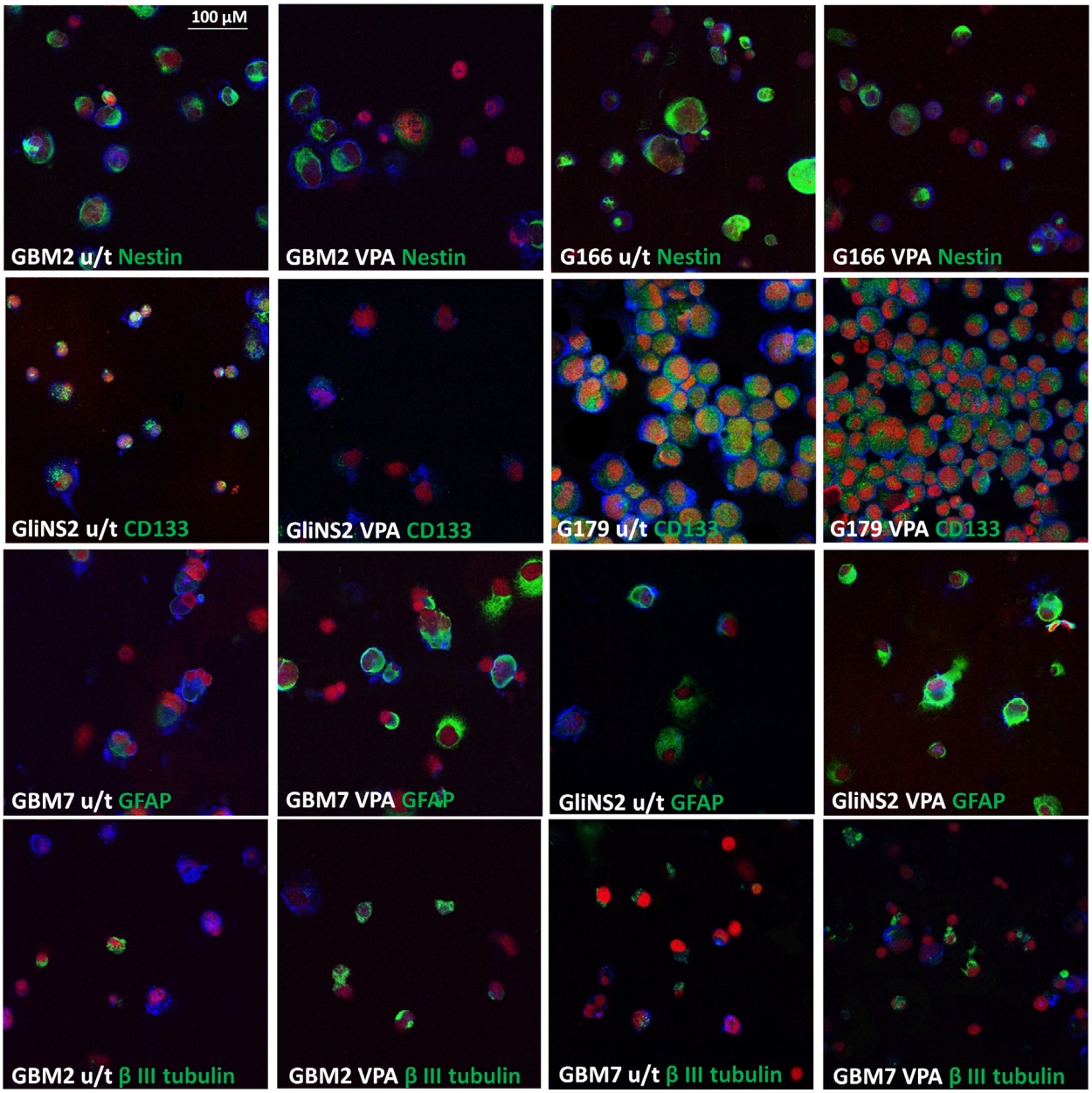

Fig. 4. Selected representative images of immunofluorescence on untreated (u/t) GSCs and 2 mM VPA treated GSCs (+VPA) for 72hs (spotted on glass slides using cytospin). Each specific maker is in green; phalloidin is in blue and propidium iodide in red. Scale bar = 100 µm.

for at least one stemness marker in 4/6 lines. GBM2 and G166 cell lines showed a decrease in Nestin immunoreactive cells from 75.4% to 53.8% and from 78.3% to 53.7%, respectively. Both cell lines displayed also a decrease in CD133 positive cells, but this variation was not statistically significant. VPA treatment on GliNS2 line induced a reduction of CD133 expression of approximately a half, from 100% to 55.5%. In G179 cell line, Nestin expression was relatively preserved after drug treatment, whereas a little decrease (but not statistically significant) in CD133 expression was observed. Surprisingly, GBM7 cell line showed an increased expression of Nestin after VPA treatment. After VPA administration, three cell lines (GBM2, GBM7 and G166) exhibited a progressive enrichment in cells expressing βIII tubulin, indicating the capability of these cells to move toward neuronal differentiation. In addition, GBM7 cell line showed an increased expression of GFAP positive cells. On the contrary, G144 cell line manifested a reduction of βIII tubulin-positive cells. The other cell lines did not show any variation in differentiation marker expression, maybe due to the high expression rate observed also in untreated cells. Unfortunately, MBP immunostaining was not informative, as its expression remained constant after treatment (Table S3, Fig. 4).

Supplementary Table 3 can be found, in the online version, at doi:10.1016/j.toxrep.2014.05.005.

3.7. Effect of VPA-PTX combined treatment on cell viability

The most effective therapeutic approach to cancer requires, for the majority of patients, the administration of a combination of drugs, in the context of specific multimodal chemotherapies with different molecular targets.

In this study, we tested the effect of VPA plus PTX combined treatment on GSC viability by MTT assay. The proposed therapeutic strategy contemplates an epigenetic switch triggered by VPA, which could modify the stem-like features of GSCs, inducing a differentiation-like process, followed by a PTX exposure. In particular, GSCs were treated with VPA 24 h before PTX administration; then, VPA and PTX were incubated together for further 48 h and subsequently cell viability was assessed *via* MTT assay (Fig. S1B). The rationale for the time-scheduled administration of VPA prior to PTX was related to the differentiation induction triggered by the former (as evidenced by the morphologic analysis) and the inhibition of cell proliferation, through cell cycle arrest and induction of apoptosis, caused by the latter. Pretreatment of the cells with different concentrations of VPA significantly increased PTX effects (Fig. 5). However, since the sensitivity to the combined treatment varied among the GSC lines, its effect was evaluated through the cooperative index (CI) [1] (Table S4).

Supplementary Table 4 can be found, in the online version, at doi:10.1016/j.toxrep.2014.05.005.

G166 cell line was the least sensitive to the combined treatment, which resulted antagonistic in the majority of dose combinations; in particular, a synergistic effect was noticed only combining the highest concentrations of PTX (10–20-50 μM) and VPA (6–10 mM). GBM2, GBM7, G144, G179 and GliNS2 cell lines showed a different pattern of viability inhibition after the coupled administration. Generally, a marked synergistic effect of VPA and PTX was noticed at the lowest doses of VPA (0.5 and 1 mM), regardless of PTX concentration. Specifically, GBM7 and G144 cell lines also displayed a significant increase in cell death combining the highest doses of both drugs (6–10 mM VPA plus 50 μM PTX and 6–10 mM VPA plus 20–50 μM PTX, respectively). Moreover, the effect of the dual treatment was significant at 6 mM VPA plus 20–50 μM PTX for G179 and 10 mM VPA plus 50 μM PTX for GliNS2. Lastly, GBM2 cell line reached a 70% reduction in cell viability even at the lowest doses of VPA and PTX (0.5 mM VPA and 0.1 μM PTX). This effect was obtained by 6 mM VPA alone, whereas PTX treatment, even at high doses, was unable to induce such an effect.

To determine the real effectiveness of the time-scheduled treatment (VPA exposure before PTX treatment), cell viability was evaluated also with the opposite arrangement. For this purpose, PTX 1 μM was administered to GBM2 and G144 cell lines 24 h before VPA treatment and the combined analysis revealed no additive or synergistic effect (data not shown, CI values reported in Table S4), suggesting that the efficacy of the dual treatment is associated with the administration timing and with the specific biological effect of each drug.

4. Discussion

Cultured GSC lines are a valuable model for testing drug susceptibility. The genomic profiles of the 6 GSC lines used in this work were extensively characterized in a previous work by our research group [2]. Briefly, the GSCs lines showed considerable karyotypic variability. The modal number of chromosomes spans from near-diploid to near-pentaploid. Each cell line shows a complex karyotype composed of both structural and numerical abnormalities. The most common numerical aberration was gain of whole chr 7, that was observed in the 70% of analyzed metaphases. Other commonly observed numerical changes are loss of chr 13 (43%), loss of sexual chromosomes (chr X 28% and chr Y 39%) and loss of chr 10 (32%, 3 out of 6 lines). Chromosome 1 was the most frequently involved in structural abnormalities (6/6 lines). Also chr 11 (3/6 lines), 18 and 12 (4/6 lines) were often rearranged. Moreover, chr 6 showed deletions or translocations involving the long arm in 3 out of 6 lines. Array CGH analysis showed some common genomic features in GSCs, such as loss of 9p21.3 locus (4/6 cell lines), that harbors CDKN2A and CDKN2B genes, pseudomonosomy for whole chr 10 (3/6 lines), with the consequent absence of PTEN gene, and complete or partial gain of chr 7 (4/6 lines), which contains EGFR gene.

Identifying a suitable approach for the eradication of the stem cell subpopulation of glioma is essential to achieve an effective treatment for GBM. In order to evaluate the therapeutic efficacy of a drug, it is appropriate to assess different biological parameters, in order to have a comprehensive view on the cellular action of the compound of interest. In this study we analyzed the variations of two cytogenetic parameters (polymorphic nuclei and mitotic index) caused by VPA or PTX administration and we performed a cell viability study by MTT assay after single and combined treatment with the two drugs, to detect a potential reduction in proliferation and an effective cytotoxicity on cancer cells. This approach requires the formulation of a solid method for the integration of data with various biological nature in order to interpret them together, specifically obtaining a global evaluation of drug efficacy.

Valproic acid (VPA) induces differentiation of several types of cancer cells, both *in vitro* and *in vivo* [11,10] and it is able to permeate the blood brain barrier (BBB), with minimal toxicity profile, even after chronic treatment, thus representing an attractive agent for cancer treatment [44,56]. Several studies were conducted to characterize the *in vitro* neurotoxicological impact of VPA. In 1998, Fennrich and collegues demonstrated that 2.5 mM and 5 mM VPA cause toxic effects on organotipically cultured hippocampi by affecting specific populations of astrocytes [18]. Moreover, Wang and collegues showed that 1 mM VPA exposure for 7 days induces a weak increase of apoptotic cells in neuron-enriched cultures, while 0.25–1 mM VPA selectively causes neuronal apoptosis in a neuron–astrocyte mixed cell culture, suggesting a synergism between the two cell types [60]. In our study, VPA inhibited cell growth in a dose- and time-dependent manner in all the GSC lines.

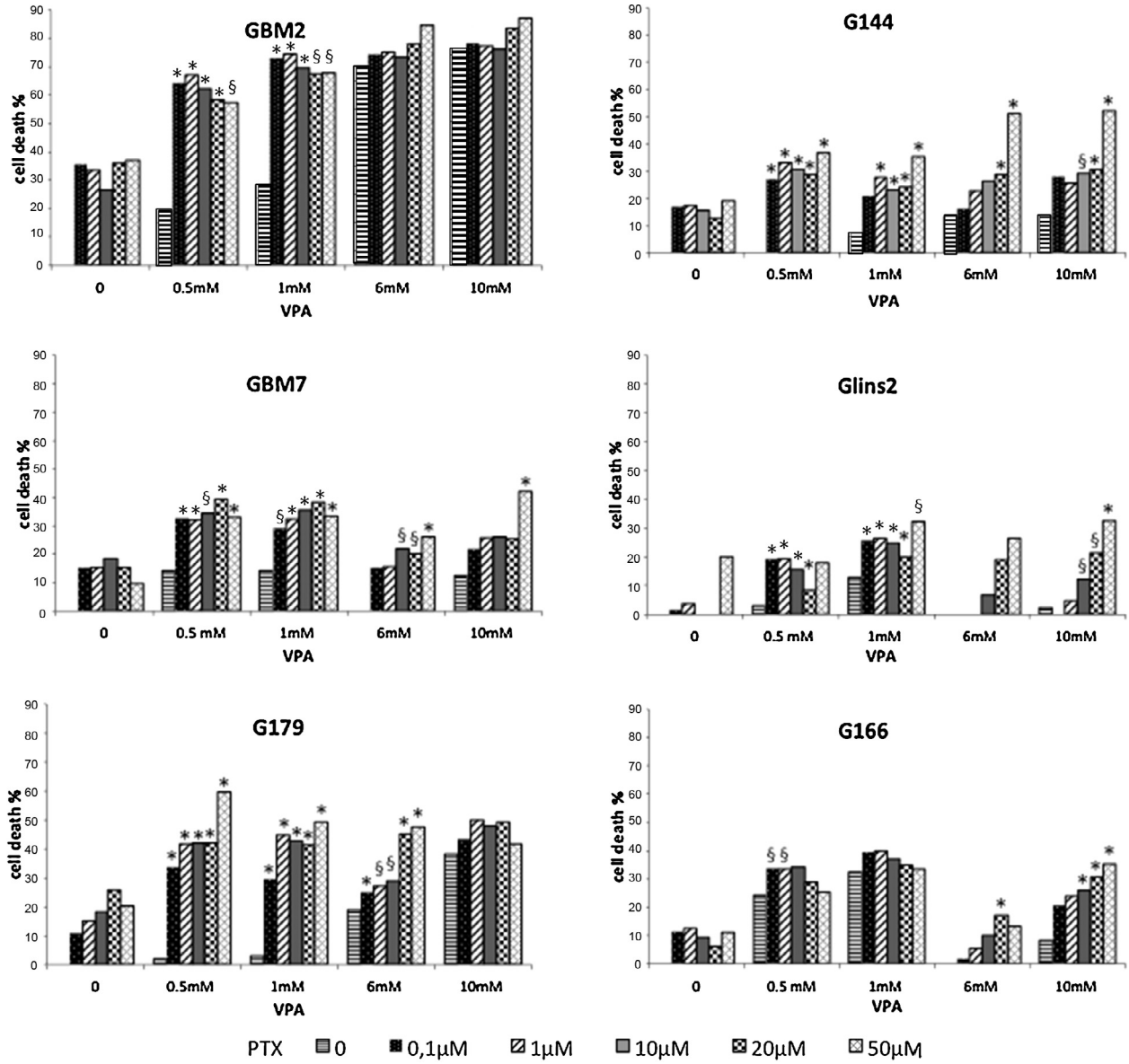

Fig. 5. Cell viability assays on GSC lines using VPA and PTX in combined treatment. Cell viability was measured as percentage of cell survival in drug-treated cells relative to untreated cells. We show mortality percentages. Results are reported as means from two different experiments performed at least in triplicate. Standard error of the mean (SEM) was constantly lower than 5% of each mean value. *CI < 1, synergistic effect; §CI = 1, additive effect.

VPA is able to modify the expression of genes involved in cell cycle, differentiation, DNA repair and apoptosis [49,54]. Specifically, it stimulates p21 expression, inducing G1/S block of cell cycle [9], and simultaneously activates apoptotic program, through the down-regulation of anti-apoptotic proteins, such as Bcl-2/Bcl-XL [67,32]. Indeed, we observed a mitotic index decrease after drug treatment, confirming a G1 block induced by VPA [46,42]. Moreover, VPA reduced the chromosome number scattering and selectively depleted polyploid cells: only cells with a lower number of chromosome were able to continue in the cell cycle, whereas the others were negatively selected (data not shown). This behavior can be translated into a change in nuclear morphology compared to untreated cells, as also described by [30]. Probably, VPA induced a decrease in cell viability by inhibition of cell proliferation and induction of differentiation, rather than by apoptosis [23]. Generally, cells arrested in G1 phase evolve toward differentiation and this process is mutually exclusive with apoptosis [4]. Anyway, the factors determining cell fate (cycle arrest, differentiation or apoptosis) are still unknown. Afterwards, we demonstrated that VPA treatment strongly modifies cellular morphology and expression of stemness (CD133 and Nestin) and differentiation (GFAP, βIII-tubulin and MBP) markers in all the GSC lines. Although with a remarkable interlinear variability, VPA triggered a differentiation-like process, which may reflect the differentiative potential or the differentiation

block of each cell line. Regarding the VPA responsivity score, we suggested the good efficacy of this drug, allowing us to classify GSC lines from the most sensitive to the least responsive: G166, G179 and G144, GBM2, GBM7, GliNS2.

Paclitaxel (PTX) is a mitotic inhibitor, which binds to the β-subunit of tubulin in microtubules, stabilizing their dynamics, leading to mitotic arrest and apoptosis [27]. In our study PTX had a weak effect on GSC lines and only GBM2 cell line showed a considerable decrease in cell viability after 72 h exposure. PTX treatment is able to induce a G2/M block, which leads to the accumulation of mitotic figures, increasing the mitotic index, as an expected consequence [55]. The induction of mitotic arrest is the primary mechanism of action of drugs affecting microtubule dynamics [22]. Cells remained in mitosis for up to 24 h and then attempted to complete mitosis, however cytokynesis remained inhibited and cells became multinucleated or polyploid, as also described by Liebmann and collegues in 1994. Escaping from mitosis and entering interphase is termed "mitotic slippage" [16] and it induces a multinucleated grape-like nuclear morphology of slipped cells, identified as an increased percentages of polymorphic nuclei, as already highlighted by [48]. After 48 h treatment, the percentage of mitotic cells decreased, showing that the initially blocked cells attempt to complete mitosis. Cells escaping mitotic block bypass cellular division and this process results in endoreduplication and, consequently, polyploidization [33]. Subsequently, these cells undergo a non-apoptotic form of cell death, known as mitotic catastrophe [17]. Cells insensitive to PTX treatment may have mutations in genes involved in the mitotic checkpoint, which accelerate mitotic process and reduce mitosis length: in 2009, Yang and collegues demonstrated that these cells did not show accumulation of mitotic figures after PTX treatment for 24 h [64]. The decrease of mitotic index in barely sensitive cells may be linked to a general induction of apoptosis by PTX, that may occur *via* signaling pathways independent from mitotic arrest [8]. The variability in response to mitotic stress in GSC lines reflects their differential sensitivity to drug treatment and cytomorphological parameters may represent an important indicator of pathological response to drug administration [7]. PTX is extensively used in several types of solid cancer [50] and it has been recently shown to have a therapeutic effect both *in vitro* on glioma cells [66] and *in vivo* on GBM xenografts in mice [28,29]. The weak permeability of PTX to the BBB may be a limiting aspect in clinical practice, anyway BBB integrity is often compromised in GBM patient, the blood capillaries are leaky [12] and moreover, several strategies to improve PTX delivery in the brain, such as the use of engineered nanoparticles, are under investigations [63].

With regard to PTX responsivity score, we noted the limited effectiveness of this drug on the GSC lines tested (except for G179 line), bearing witness to the high chemoresistance of GBM. This behavior could be related to the partial or complete gain of chromosome 7 in all the GSC lines of the study [2]. Indeed, at 7p22.3 is mapped MAD1L1 gene, a component of mitotic checkpoint, which is able to confer chemoresistance to microtubule poisons, such as PTX, when up-regulated [52].

To overcome the limitations linked to a single agent therapy, we decided to combine VPA and PTX in order to verify the effect of this dual treatment on GSC viability. We utilized VPA as a sensitizer agent in order to improve the PTX effectiveness through the induction of differentiation triggered by HDAC inhibitors [14]. Specifically, differentiation-inducing therapies are the most promising treatments, in order to affect the self-renewal ability of the cancer stem cell subpopulation. The ability of VPA to induce differentiation is the rationale for its use in a combined treatment: the induction of GSC differentiation and the reduction of cell proliferation can be coupled with a drug able to promote cell death, such as PTX [51]. After VPA induced-differentiation, PTX might be able to influence cell viability of cells downstream in the hierarchical composition of GBM. Globally, cell death was increased after dual treatment in all the GSC lines, thus VPA enhanced the anticancer action in combination with PTX. Five cell lines (GBM2, GBM7, G144, G179, GliNS2) showed an increased synergism at lower concentrations of both drugs: when using lower doses, toxicity can be minimized and therapeutic efficacy maintained. This approach is strictly dependent on time-scheduled administration: reverse treatment, indeed, did not display any synergism. The clinical use of PTX is hampered by its severe side effects [6], but they are chiefly dependent upon high dose regimens and on Cremophor EL, which is used as vehicle [43]. In particular, PTX neurotoxicity is caused by the disruption of microtubule structure and axonal degeneration, that lead to the impairment of the axoplasmic transport: LaPointe and collegues reported that a 10 μM PTX dose is able to induce such effect [34]. Ustinova and collaborators demonstrated that 0.1 nM and 0.5 nM PTX do not influence the neuronal growth in cultures, but higher concentrations of PTX (1–10–100 nM) have significant toxic effects on murine dorsal root ganglion neurons [59]. VPA administration may consent the reduction of PTX concentration, maintaining the same killing effect and allowing an effective treatment [5]. The effectiveness of VPA combined with PTX administration was due to the ability of VPA to enhance the sensitivity to chemotherapeutic agents [41]. Alternatively, since VPA induces α tubulin acetylation [5], which could suppresses microtubule dynamics, VPA may positively affect PTX binding to microtubules.

Collectively, the combination of VPA and PTX could be a real potential therapeutic strategy to specifically eradicate GSCs and might provide insights for the design of new clinical treatments of GBM. Lastly, our multiple drug responsivity assay could represent a useful tool to assess the efficacy of different antineoplastic drugs because it relies on the evaluation of multiple cell parameters, whose results are in this way integrated; in the future, this method could help to select the right treatment and to perform optimal drug combinations.

Funding

This work was supported by FAR 2011 no. 12-1-62 and no. 12-155 from University of Milano-Bicocca (to LD and

AB, respectively) and by FIRB project from Ministry of University and Scientific Research (to ML).

Conflict of interests

The authors disclose any actual or potential conflict of interest in relation to this article.

Transparency document

The Transparency document associated with this article can be found in the online version.

Acknowledgment

The authors want to gratefully acknowledge Professor Austin Smith (Wellcome Trust-Medical Research Council Stem Cell Institute, University of Cambridge, Cambridge UK) and Isenet (http://www.isenet.it/index.php/eu) for kindly providing us with the cell lines used in this study. The authors also want to thank Dr. Laura Antolini for her professional assistance.

References

[1] N. Aouali, V. Palissot, V. El-Khoury, E. Moussay, B. Janji, S. Pierson, N.H. Brons, L. Kellner, M. Bosseler, K. Van Moer, G. Berchem, Peroxisome proliferator-activated receptor gamma agonists potentiate the cytotoxic effect of valproic acid in multiple myeloma cells, Br. J. Haematol. 147 (2009) 662–671.

[2] S. Baronchelli, A. Bentivegna, S. Redaelli, G. Riva, V. Butta, L. Paoletta, G. Isimbaldi, M. Miozzo, S. Tabano, A. Daga, D. Marubbi, M. Cattaneo, I. Biunno, L. Dalprà, Delineating the cytogenomic and epigenomic landscapes of glioma stem cell lines, PLoS ONE 8 (2013) e57462.

[3] J. Barretina, G. Caponigro, N. Stransky, K. Venkatesan, A.A. Margolin, S. Kim, C.J. Wilson, J. Lehár, G.V. Kryukov, D. Sonkin, A. Reddy, M. Liu, L. Murray, M.F. Berger, J.E. Monahan, P. Morais, J. Meltzer, A. Korejwa, J. Jané-Valbuena, F.A. Mapa, J. Thibault, E. Bric-Furlong, P. Raman, A. Shipway, I.H. Engels, J. Cheng, G.K. Yu, J. Yu, P. Aspesi, M. de Silva, K. Jagtap, M.D. Jones, L. Wang, C. Hatton, E. Palescandolo, S. Gupta, S. Mahan, C. Sougnez, R.C. Onofrio, T. Liefeld, L. MacConaill, W. Winckler, M. Reich, N. Li, J.P. Mesirov, S.B. Gabriel, G. Getz, K. Ardlie, V. Chan, V.E. Myer, B.L. Weber, J. Porter, M. Warmuth, P. Finan, J.L. Harris, M. Meyerson, T.R. Golub, M.P. Morrissey, W.R. Sellers, R. Schlegel, L.A. Garraway, The Cancer Cell Line Encyclopedia enables predictive modelling of anticancer drug sensitivity, Nature 483 (2012) 603–607.

[4] M.G. Catalano, N. Fortunati, M. Pugliese, L. Costantino, R. Poli, O. Bosco, G. Boccuzzi, Valproic acid induces apoptosis and cell cycle arrest in poorly differentiated thyroid cancer cells, J. Clin. Endocrinol. Metab. 90 (2005) 1383–1389.

[5] M.G. Catalano, R. Poli, M. Pugliese, N. Fortunati, G. Boccuzzi, Valproic acid enhances tubulin acetylation and apoptotic activity of paclitaxel on anaplastic thyroid cancer cell lines, Endocr. Relat. Cancer 14 (2007) 839–845.

[6] G. Cavaletti, G. Tredici, M. Braga, S. Tazzari, Experimental peripheral neuropathy induced in adult rats by repeated intraperitoneal administration of taxol, Exp. Neurol. 133 (1995) 64–72.

[7] A.B. Chakravarthy, M.C. Kelley, B. McLaren, C.I. Truica, D. Billheimer, I.A. Mayer, A.M. Grau, D.H. Johnson, J.F. Simpson, R.D. Beauchamp, C. Jones, J.A. Pietenpol, Neoadjuvant concurrent paclitaxel and radiation in stage II/III breast cancer, Clin. Cancer Res. 12 (2006) 1570–1576.

[8] J.G. Chen, S.B. Horwitz, Differential mitotic responses to microtubule-stabilizing and -destabilizing drugs, Cancer Res. 62 (2002) 1935–1938.

[9] Y.C. Cheng, H. Lin, M.J. Huang, J.M. Chow, S. Lin, H.E. Liu, Downregulation of c-Myc is critical for valproic acid-induced growth arrest and myeloid differentiation of acute myeloid leukemia, Leuk. Res. 31 (2007) 1403–1411.

[10] J. Cinatl, P.H. Driever, R. Kotchetkov, P. Pouckova, B. Kornhuber, D. Schwabe, Sodium valproate inhibits in vivo growth of human neuroblastoma cells, Anticancer Drugs 8 (1997) 958–963.

[11] J. Cinatl, M. Scholz, P.H. Driever, D. Henrich, H. Kabickova, J.U. Vogel, H.W. Doerr, B. Kornhuber, Antitumor activity of sodium valproate in cultures of human neuroblastoma cells, Anticancer Drugs 7 (1996) 766–773.

[12] B.L. Coomber, P.A. Stewart, K. Hayakawa, C.L. Farrell, R.F. Del Maestro, Quantitative morphology of human glioblastoma multiforme microvessels: structural basis of blood-brain barrier defect, J. Neurooncol. 5 (1987) 299–307.

[13] J. Crown, M. O'Leary, The taxanes: an update, Lancet 355 (2000) 1176–1178.

[14] F.D. Cruz, I. Matushansky, Solid tumor differentiation therapy – is it possible? Oncotarget 3 (2012) 559–567.

[15] A. Duenas-Gonzalez, M. Candelaria, C. Perez-Plascencia, E. Perez-Cardenas, E. de la Cruz-Hernandez, L.A. Herrera, Valproic acid as epigenetic cancer drug: preclinical, clinical and transcriptional effects on solid tumors, Cancer Treat. Rev. 34 (2008) 206–222.

[16] A. Elhajouji, M. Cunha, M. Kirsch-Volders, Spindle poisons can induce polyploidy by mitotic slippage and micronucleate mononucleates in the cytokinesis-block assay, Mutagenesis 13 (1998) 193–198.

[17] J.E. Erenpreisa, A. Ivanov, G. Dekena, A. Vitina, R. Krampe, T. Freivalds, G. Selivanova, H.I. Roach, Arrest in metaphase and anatomy of mitotic catastrophe: mild heat shock in two human osteosarcoma cell lines, Cell Biol. Int. 24 (2000) 61–70.

[18] S. Fennrich, D. Ray, H. Nau, B. Schlosshauer, Radial astrocytes: toxic effects induced by antiepileptic drug in the developing rat hippocampus in vitro, Eur. J. Cell Biol. 77 (1998) 142–150.

[19] M.J. Garnett, E.J. Edelman, S.J. Heidorn, C.D. Greenman, A. Dastur, K.W. Lau, P. Greninger, I.R. Thompson, X. Luo, J. Soares, Q. Liu, F. Iorio, D. Surdez, L. Chen, R.J. Milano, G.R. Bignell, A.T. Tam, H. Davies, J.A. Stevenson, S. Barthorpe, S.R. Lutz, F. Kogera, K. Lawrence, A. McLaren-Douglas, X. Mitropoulos, T. Mironenko, H. Thi, L. Richardson, W. Zhou, F. Jewitt, T. Zhang, P. O'Brien, J.L. Boisvert, S. Price, W. Hur, W. Yang, X. Deng, A. Butler, H.G. Choi, J.W. Chang, J. Baselga, I. Stamenkovic, J.A. Engelman, S.V. Sharma, O. Delattre, J. Saez-Rodriguez, N.S. Gray, J. Settleman, P.A. Futreal, D.A. Haber, M.R. Stratton, S. Ramaswamy, U. McDermott, C.H. Benes, Systematic identification of genomic markers of drug sensitivity in cancer cells, Nature 483 (2012) 570–575.

[20] F. Griffero, A. Daga, D. Marubbi, M.C. Capra, A. Melotti, A. Pattarozzi, M. Gatti, A. Bajetto, C. Porcile, F. Barbieri, R.E. Favoni, M. Lo Casto, G. Zona, R. Spaziante, T. Florio, G. Corte, Different response of human glioma tumor-initiating cells to epidermal growth factor receptor kinase inhibitors, J. Biol. Chem. 284 (2009) 7138–7148.

[21] B. Haibe-Kains, N. El-Hachem, N.J. Birkbak, A.C. Jin, A.H. Beck, H.J. Aerts, J. Quackenbush, Inconsistency in large pharmacogenomic studies, Nature 504 (2013) 389–393.

[22] S.B. Horwitz, Mechanism of action of taxol, Trends Pharmacol. Sci. 13 (1992) 134–136.

[23] A. Hrzenjak, F. Moinfar, M.L. Kremser, B. Strohmeier, P.B. Staber, K. Zatloukal, H. Denk, Valproate inhibition of histone deacetylase 2 affects differentiation and decreases proliferation of endometrial stromal sarcoma cells, Mol. Cancer Ther. 5 (2006) 2203–2210.

[24] T.N. Ignatova, V.G. Kukekov, E.D. Laywell, O.N. Suslov, F.D. Vrionis, D.A. Steindler, Human cortical glial tumors contain neural stem-like cells expressing astroglial and neuronal markers in vitro, Glia 39 (2002) 193–206.

[25] Y. Iwadate, S. Fujimoto, M. Tagawa, H. Namba, K. Sueyoshi, M. Hirose, S. Sakiyama, Association of p53 gene mutation with decreased chemosensitivity in human malignant gliomas, Int. J. Cancer 69 (1996) 236–240.

[26] Y. Iwadate, S. Mochizuki, S. Fujimoto, H. Namba, S. Sakiyama, M. Tagawa, A. Yamaura, Alteration of CDKN2/p16 in human astrocytic tumors is related with increased susceptibility to antimetabolite anticancer agents, Int. J. Oncol. 17 (2000) 501–505.

[27] M.A. Jordan, K. Wendell, S. Gardiner, W.B. Derry, H. Copp, L. Wilson, Mitotic block induced in HeLa cells by low concentrations of paclitaxel (Taxol) results in abnormal mitotic exit and apoptotic cell death, Cancer Res. 56 (1996) 816–825.

[28] S. Karmakar, N.L. Banik, S.J. Patel, S.K. Ray, Combination of all-trans retinoic acid and taxol regressed glioblastoma T98G xenografts in nude mice, Apoptosis 12 (2007) 2077–2087.

[29] S. Karmakar, N.L. Banik, S.K. Ray, Combination of all-trans retinoic acid and paclitaxel-induced differentiation and apoptosis in human glioblastoma U87MG xenografts in nude mice, Cancer 112 (2008) 596–607.

[30] M.S. Kortenhorst, S. Isharwal, P.J. van Diest, W.H. Chowdhury, C. Marlow, M.A. Carducci, R. Rodriguez, R.W. Veltri, Valproic acid causes dose- and time-dependent changes in nuclear structure in prostate cancer cells in vitro and in vivo, Mol. Cancer Ther. 8 (2009) 802–808.

[31] M. Krajcovic, M. Overholtzer, Mechanisms of ploidy increase in human cancers: a new role for cell cannibalism, Cancer Res. 72 (2012) 1596–1601.
[32] L. Lagneaux, N. Gillet, B. Stamatopoulos, A. Delforge, M. Dejeneffe, M. Massy, N. Meuleman, A. Kentos, P. Martiat, L. Willems, D. Bron, Valproic acid induces apoptosis in chronic lymphocytic leukemia cells through activation of the death receptor pathway and potentiates TRAIL response, Exp. Hematol. 35 (2007) 1527–1537.
[33] C. Lanzi, G. Cassinelli, G. Cuccuru, R. Supino, V. Zuco, C. Ferlini, G. Scambia, F. Zunino, Cell cycle checkpoint efficiency and cellular response to paclitaxel in prostate cancer cells, Prostate 48 (2001) 254–264.
[34] N.E. LaPointe, G. Morfini, S.T. Brady, S.C. Feinstein, L. Wilson, M.A. Jordan, Effects of eribulin, vincristine, paclitaxel and ixabepilone on fast axonal transport and kinesin-1 driven microtubule gliding: implications for chemotherapy-induced peripheral neuropathy, Neurotoxicology 37 (2013) 231–239.
[35] J. Lee, S. Kotliarova, Y. Kotliarov, A. Li, Q. Su, N.M. Donin, S. Pastorino, B.W. Purow, N. Christopher, W. Zhang, J.K. Park, H.A. Fine, Tumor stem cells derived from glioblastomas cultured in bFGF and EGF more closely mirror the phenotype and genotype of primary tumors than do serum-cultured cell lines, Cancer Cell 9 (2006) 391–403.
[36] G.H. Li, H. Wei, Z.T. Chen, S.Q. Lv, C.L. Yin, D.L. Wang, STAT3 silencing with lentivirus inhibits growth and induces apoptosis and differentiation of U251 cells, J. Neurooncol. 91 (2009) 165–174.
[37] X.N. Li, Q. Shu, J.M. Su, L. Perlaky, S.M. Blaney, C.C. Lau, Valproic acid induces growth arrest, apoptosis, and senescence in medulloblastomas by increasing histone hyperacetylation and regulating expression of p21Cip1, CDK4, and CMYC, Mol. Cancer Ther. 4 (2005) 1912–1922.
[38] G. Liu, X. Yuan, Z. Zeng, P. Tunici, H. Ng, I.R. Abdulkadir, L. Lu, D. Irvin, K.L. Black, J.S. Yu, Analysis of gene expression and chemoresistance of CD133+ cancer stem cells in glioblastoma, Mol. Cancer 5 (2006) 67.
[39] N.A. Lobo, Y. Shimono, D. Qian, M.F. Clarke, The biology of cancer stem cells, Annu. Rev. Cell Dev. Biol. 23 (2007) 675–699.
[40] D.N. Louis, H. Ohgaki, O.D. Wiestler, W.K. Cavenee, P.C. Burger, A. Jouvet, B.W. Scheithauer, P. Kleihues, The 2007 WHO classification of tumours of the central nervous system, Acta Neuropathol. 114 (2007) 97–109.
[41] A. Mai, L. Altucci, Epi-drugs to fight cancer: from chemistry to cancer treatment, the road ahead, Int. J. Biochem. Cell Biol. 41 (2009) 199–213.
[42] M.L. Martin, K.C. Breen, C.M. Regan, Perturbations of cellular functions integral to neural tube formation by the putative teratogen sodium valproate, Toxicol. In Vitro 2 (1988) 43–48.
[43] S. Mielke, A. Sparreboom, K. Mross, Peripheral neuropathy: a persisting challenge in paclitaxel-based regimes, Eur. J. Cancer 42 (2006) 24–30.
[44] E. Perucca, Pharmacological and therapeutic properties of valproate: a summary after 35 years of clinical experience, CNS Drugs 16 (2002) 695–714.
[45] S.M. Pollard, K. Yoshikawa, I.D. Clarke, D. Danovi, S. Stricker, R. Russell, J. Bayani, R. Head, M. Lee, M. Bernstein, J.A. Squire, A. Smith, P. Dirks, Glioma stem cell lines expanded in adherent culture have tumor-specific phenotypes and are suitable for chemical and genetic screens, Cell Stem Cell 4 (2009) 568–580.
[46] C.M. Regan, Therapeutic levels of sodium valproate inhibit mitotic indices in cells of neural origin, Brain Res. 347 (1985) 394–398.
[47] T. Reya, S.J. Morrison, M.F. Clarke, I.L. Weissman, Stem cells, cancer, and cancer stem cells, Nature 414 (2001) 105–111.
[48] J.L. Riffell, C. Zimmerman, A. Khong, L.M. McHardy, M. Roberge, Effects of chemical manipulation of mitotic arrest and slippage on cancer cell survival and proliferation, Cell Cycle 8 (2009) 3025–3038.
[49] R.R. Rosato, J.A. Almenara, Y. Dai, S. Grant, Simultaneous activation of the intrinsic and extrinsic pathways by histone deacetylase (HDAC) inhibitors and tumor necrosis factor-related apoptosis-inducing ligand (TRAIL) synergistically induces mitochondrial damage and apoptosis in human leukemia cells, Mol. Cancer Ther. 2 (2003) 1273–1284.
[50] E.K. Rowinsky, M. Wright, B. Monsarrat, G.J. Lesser, R.C. Donehower, Taxol: pharmacology, metabolism and clinical implications, Cancer Surv. 17 (1993) 283–304.
[51] S. Roy Choudhury, S. Karmakar, N.L. Banik, S.K. Ray, Valproic acid induced differentiation and potentiated efficacy of taxol and nanotaxol for controlling growth of human glioblastoma LN18 and T98G cells, Neurochem. Res. 36 (2011) 2292–2305.
[52] S.D. Ryan, E.M. Britigan, L.M. Zasadil, K. Witte, A. Audhya, A. Roopra, B.A. Weaver, Up-regulation of the mitotic checkpoint component Mad1 causes chromosomal instability and resistance to microtubule poisons, Proc. Natl. Acad. Sci. U.S.A. 109 (2012) E2205–E2214.
[53] E. Sachlos, R.M. Risueño, S. Laronde, Z. Shapovalova, J.H. Lee, J. Russell, M. Malig, J.D. McNicol, A. Fiebig-Comyn, M. Graham, M. Levadoux-Martin, J.B. Lee, A.O. Giacomelli, J.A. Hassell, D. Fischer-Russell, M.R. Trus, R. Foley, B. Leber, A. Xenocostas, E.D. Brown, T.J. Collins, M. Bhatia, Identification of drugs including a dopamine receptor antagonist that selectively target cancer stem cells, Cell 149 (2012) 1284–1297.
[54] J. Savickiene, V.V. Borutinskaite, G. Treigyte, K.E. Magnusson, R. Navakauskiene, The novel histone deacetylase inhibitor BML-210 exerts growth inhibitory, proapoptotic and differentiation stimulating effects on the human leukemia cell lines, Eur. J. Pharmacol. 549 (2006) 9–18.
[55] D.M. Scolnick, T.D. Halazonetis, Chfr defines a mitotic stress checkpoint that delays entry into metaphase, Nature 406 (2000) 430–435.
[56] W.T. Shen, T.S. Wong, W.Y. Chung, M.G. Wong, E. Kebebew, Q.Y. Duh, O.H. Clark, Valproic acid inhibits growth, induces apoptosis, and modulates apoptosis-regulatory and differentiation gene expression in human thyroid cancer cells, Surgery 138 (2005) 979–984, discussion 984–985.
[57] S.K. Singh, C. Hawkins, I.D. Clarke, J.A. Squire, J. Bayani, T. Hide, R.M. Henkelman, M.D. Cusimano, P.B. Dirks, Identification of human brain tumour initiating cells, Nature 432 (2004) 396–401.
[58] S.H. Stricker, A. Feber, P.G. Engström, H. Carén, K.M. Kurian, Y. Takashima, C. Watts, M. Way, P. Dirks, P. Bertone, A. Smith, S. Beck, S.M. Pollard, Widespread resetting of DNA methylation in glioblastoma-initiating cells suppresses malignant cellular behavior in a lineage-dependent manner, Genes Dev. 27 (2013) 654–669.
[59] E.E. Ustinova, G.V. Shurin, D.W. Gutkin, M.R. Shurin, The role of TLR4 in the paclitaxel effects on neuronal growth in vitro, PLoS ONE 8 (2013) e56886.
[60] C. Wang, Z. Luan, Y. Yang, Z. Wang, Y. Cui, G. Gu, Valproic acid induces apoptosis in differentiating hippocampal neurons by the release of tumor necrosis factor-α from activated astrocytes, Neurosci. Lett. 497 (2011) 122–127.
[61] J.N. Weinstein, P.L. Lorenzi, Cancer: discrepancies in drug sensitivity, Nature 504 (2013) 381–383.
[62] P.Y. Wen, S. Kesari, Malignant gliomas in adults, N. Engl. J. Med. 359 (2008) 492–507.
[63] D. Yang, S. Van, X. Jiang, L. Yu, Novel free paclitaxel-loaded poly(L-(-glutamylglutamine)-paclitaxel nanoparticles, Int. J. Nanomed. 6 (2011) 85–91.
[64] Z. Yang, A.E. Kenny, D.A. Brito, C.L. Rieder, Cells satisfy the mitotic checkpoint in Taxol, and do so faster in concentrations that stabilize syntelic attachments, J. Cell Biol. 186 (2009) 675–684.
[65] W.K. Yung, J.R. Shapiro, W.R. Shapiro, Heterogeneous chemosensitivities of subpopulations of human glioma cells in culture, Cancer Res. 42 (1982) 992–998.
[66] R. Zhang, N.L. Banik, S.K. Ray, Differential sensitivity of human glioblastoma LN18 (PTEN-positive) and A172 (PTEN-negative) cells to Taxol for apoptosis, Brain Res. 1239 (2008) 216–225.
[67] M.F. Ziauddin, W.S. Yeow, J.B. Maxhimer, A. Baras, A. Chua, R.M. Reddy, W. Tsai, G.W. Cole, D.S. Schrump, D.M. Nguyen, Valproic acid, an antiepileptic drug with histone deacetylase inhibitory activity, potentiates the cytotoxic effect of Apo2L/TRAIL on cultured thoracic cancer cells through mitochondria-dependent caspase activation, Neoplasia 8 (2006) 446–457.